Canadian Urban Flow and Dispersion Model (CUDM)

CRTI scientific report

August 2008

A General Methodology of Urban Land Cover Type Classification for Atmospheric Modeling

A. LEMONSU[1]

Environment Canada, Meteorological Research Division, Dorval, Canada

A. LEROUX

Environment Canada, Canadian Meteorological Centre, Dorval, Canada

S. BÉLAIR

Environment Canada, Meteorological Research Division, Dorval, Canada

S. TRUDEL

Environment Canada, Canadian Meteorological Centre, Dorval, Canada

J. MAILHOT

Environment Canada, Meteorological Research Division, Dorval, Canada

[1] *Corresponding author address:* Dr. A. Lemonsu, Météo France, Centre National de Recherches Météorologiques, 42 avenue G. Coriolis, 31057 Toulouse cedex, France. E-mail: aude.lemonsu@meteo.fr

ABSTRACT

The main objective of the present work is to develop a general methodology devoted to the semi-automatic production of urban land-use land-cover (LULC) classifications for major North American cities, in order to represent the spatial distribution and diversity of urban areas in numerical atmospheric models. The method is based on the joint analysis of satellite imagery and digital elevation models (DEMs) in order to take into account the surface properties and the geometric characteristics of the urban canopy. A 15-m unsupervised classification is performed using data from the Advanced Spaceborne Thermal Emission and Reflection (ASTER) and Landsat-7 satellites. Building heights are estimated using DEMs from the Shuttle Radar Topography Mission (SRTM-DEM), National Elevation Dataset (NED), and Canadian Digital Elevation Data level 1 (CDED1). The unsupervised classification is aggregated on a 60-m grid and merged with the lower-resolution building height database. A decision-tree is then applied to allow the identification of twelve urban classes. One major advantage of this approach is the availability and low-cost of the above data, which makes possible the production of LULC classifications for all major North American cities. In this study, two application cases are presented, one for Oklahoma City (OK, United States) and another for Montreal (QC, Canada). The building heights and the LULC classification produced for Montreal are evaluated using a detailed three-dimensional building database and aerial photographs, respectively. Evaluation of the classification using aerial photographs of Montreal indicates that the LULC resulting from this approach is able to capture the main urban cover types observed in this city.

1. Introduction

In order to realistically represent surface fluxes of heat, humidity, and momemtum over cities, new urban surface schemes have recently been developed and implemented in mesoscale atmospheric models (Mills 1997; Kondo and Liu 1998; Masson 2000; Kusaka et al. 2001; Martilli et al. 2002). These schemes represent with varying degree of complexity the three-dimensional geometry of the urban canopy. The radiative and energetic exchanges are resolved by taking into account shadow effects and radiation trapping inside the streets, as well as thermal and radiative properties of the different urban facets. For instance, the Town Energy Balance scheme (TEB; Masson 2000) was recently implemented in the Global Environmental Multiscale (GEM) and the Mesoscale Compressible Community (MC2) Canadian models (Mailhot et al. 2006). The TEB specifically resolves surface energy and water exchanges over built-up areas (i.e., roads, walls, and roofs). In mixed urban environments composed of built-up (or impervious) and vegetated elements, such as residential districts, the TEB is coupled with the Interaction Soil-Biosphere-Atmosphere (ISBA; Noilhan and Planton 1989; Bélair et al. 2003) land surface scheme.

The urban canopy and land surface models require specific input data (depending on the model parameterizations) describing the built-up cover characteristics for TEB and the vegetated cover properties for ISBA. In meteorological models, they are usually defined as constant parameters associated with different classes of land use and land covers (LULC) defined in databases that are used by the models for surface mapping. Table 1 lists the TEB input parameters related to the surface characterization and to

the built-up and vegetation coverage fractions.

Currently, the GEM and MC2 atmospheric models use the 1-km grid-size global land-cover characteristics (GLCC) database (Loveland et al. 2000) consisting of twenty-six classes including water bodies, ice, and various kinds of soils and vegetation covers. Like most of the global databases (Hansen et al. 2000; Friedl et al. 2002), the GLCC database only considers one urban class, deduced from populated areas provided by the digital chart of the world (DCW; Danko 1992). In most atmospheric models, which do not include urban schemes, this single urban class is simply represented as sandy areas with large roughness. Nevertheless, more detailed urban characteristics, provided by databases with several classes, are necessary to represent the spatial variability of the landscapes at the city scale.

The environments or covers commonly referred as *urban* usually correspond to a heterogeneous arrangement of built-up elements, such as buildings, roads, or parking lots, and of vegetated covers, such as parks, trees, or courtyards. Classification of urban areas using remote sensing presents several difficulties, mostly linked to pixel mixing. For instance, mixing of various built-up elements is observed because the size of these elements is often smaller than the satellite image pixels (Ridd 1995; Lu and Weng 2004). For the same reason, there is also mixing of built-up land use and natural covers. Furthermore, urban covers as a whole have a complex three-dimensional geometry, which should be taken into account by the classification strategy. Building heights and density, as well as buildings arrangement, exhibit considerable variability and determine the dynamical roughness field (Grimmond and Oke 1999). Besides, heat storage is strongly influenced by the quantity of available surfaces (both vertical

and horizontal), which depends on the shape and density of the buildings. It is worth emphasizing, however, that the current urban LULC classifications do not consider the three-dimensional characteristics of the urban canopy.

Some LULC products already exist over Canada, such as the Canada Land Inventory (CLI), the Canadian Urban Land Use Survey (CUrLUS) and the Canada Land Use Mapping Programs (CLUMP) I and II (Guindon et al. 2004; Zhang and Guindon 2005). CUrLUS is the most recent and precise of these classifications, and includes four urban classes, i.e., *Residential*, *Commercial/Industrial*, *Urban recreational*, and *Transportation*. These classes are very similar to those found in the 30-m national land-cover data (NLCD) (Vogelmann et al. 2001) for the United States (US), derived using Landsat thematic mapper (TM) images and ancillary spatial data. Unfortunately, these urban LULC classifications do not meet TEB's requirements for urban modeling applications. The number of thematic classes is not sufficient to illustrate the urban landscape variability, in contrast for instance with what is available in Europe with the COoRdination and INformation on the Environment (CORINE) land-cover database (Heymann et al. 1993). This database provides eleven urban classes at a resolution of 100 m by coupling numerous data sources (Landsat TM and SPOT satellite images, topographic maps and aerial photographs).

Our objective in this study is thus to develop a general methodology for producing urban LULC classifications with sufficient thematic classes that can be used in atmospheric models. Because such classifications are needed for all major North American cities, a semi-automatic approach is presented, following four main steps:

1. Produce, with the best possible spatial resolution, an unsupervised classification of

built and vegetated elements, i.e., for which each pixel is associated with one dominant element.

2. Generate a database of building heights, on the same grid as 1.

3. Compute on a coarser grid (compared with the grids used in the two previous steps) the fractions of built and vegetated elements, as well as the mean building height.

4. Identify a manageable and reasonable number of urban classes (Table 2) by applying a decision tree model.

To illustrate and evaluate this methodology, two application cases are conducted for Oklahoma City (OKC) (OK, US) and Montreal (MTL, Canada). Both of these cities are representative of several North American cities: OKC is similar in size and configuration to Calgary, Winnipeg and Edmonton, i.e., cities with population of several hundreds of thousands consisting of a small central business district with skyscrapers surrounded by far-reaching residential areas, whereas MTL is similar to Toronto, Boston, Chicago, and Philadelphia, which are much larger cities with wider central business districts, which include several industrial districts, and which are surrounded by considerable residential areas.

The next section presents the source data that are used and the pre-processing applied in order to produce the unsupervised classification and the building height database. Section 3 describes the steps leading to the identification of the urban classes and Section 4 presents an evaluation of this approach against aerial photographs.

2. Source data pre-processing

a. Choice and evaluation of the source data

To speed-up the generation of urban LULC classifications for all major North American cities, the methodology should be as automatic as possible, and use the same kind of data (available for each city). Furthermore, mesoscale modeling requires urban LULC databases covering entire cities, which usually cannot easily be done with very high resolution databases such as aerial photographs (Grimmond and Souch 1994) or airborne lidar data (Burian et al. 2004) which often only cover fractions of cities. Therefore, for the present study, we chose medium-resolution satellite imagery and DEMs, which are available at low or no cost and cover large spatial areas. All the data sources used in the methodology are presented in Table 3.

The medium-resolution panchromatic and multispectral images from the Advanced Spaceborne Thermal Emission and Reflection (ASTER) and Landsat satellites, with spatial resolutions of 15-30 m, are used for the characterization of surface properties. Several examples of urban area mapping with such data have been presented for specific cities: Landsat-7 ETM+ (Stefanov et al. 2001; Lu and Weng 2004), ASTER (Ramsey 2003), Earth Observing 1 (EO-1) Advanced Land Imager (ALI), SPOT 5 HGR (De Jong et al. 2000). Even if the future of EO satellites is uncertain, it is reasonable to believe that sensors similar to those for ASTER and Landsat-7 will provide continuous data for the coming decades allowing the continuous update of the classifications.

On the other hand, the source data used in this study for the DEMs representing the Earth's topography are: (a) the Shuttle Radar Topography Mission DEM

(SRTM-DEM), a near-global database of total elevation data produced at 1 arc-second resolution (about 30 m depending on latitude) for the US and 3 arc-seconds ($\simeq$ 90 m) for the rest of the world; (b) the US Geological Survey (USGS) National Elevation Dataset (NED), which provides the bald Earth's elevation for a large part of the US with a 1/3 arc second ($\simeq$ 10 m) resolution; and (c) the Canadian Digital Elevation Data level 1 (CDED1), developed by the National Topographic DataBase (NTDB), which provides data similar to NED but at 0.75-3.00 arc-second of resolution for all Canada. Gamba et al. (2002) used SRTM-DEM minus digital terrain model data to identify buildings. When compared with classical building extraction algorithm applied to airborne TOPSAR sensor data (5-m resolution), this method was shown to be relatively successful for tall and large buildings, even though the spatial resolution is rather coarse and building heights are generally underestimated.

b. *ASTER and Landsat-7 imagery processing*

In order to allow an unsupervised classification of impervious and natural elements of cities, the ASTER satellite image of OKC (35.63 $^\circ$ N - 37.28 $^\circ$ N; 97.37 $^\circ$ W - 97.66 $^\circ$ W) with the least cloud coverage was chosen during a relatively recent summertime period (21 July 2001). The ASTER sensor consists of three separate instrument subsystems providing (a) three visible and near infrared (VNIR) bands at 15-m resolution, (b) six shortwave infrared (SWIR) bands at 30-m resolution, and (c) five thermal infrared (TIR) bands at 90-m resolution. In the current approach, only the VNIR and SWIR bands are used. Moreover, the SWIR bands are resampled (nearest neighbor) on the VNIR 15-m grid.

For Montreal, unfortunately, no recent ASTER images of acceptable quality was found, due to clouds. For this reason, the Landsat-7 image of 8 June 2001 (Table 3) is used for Montreal and its surroundings (45.33 $^\circ$N - 45.75 $^\circ$N; 74.00 $^\circ$W - 73.33 $^\circ$W). The ETM+ instrument on the Landsat-7 spacecraft contains sensors detecting: (a) six VNIR bands including one panchromatic (Pan) band, (b) two SWIR bands, and (c) one TIR band. The spatial resolutions are 15 m, 30 m and 60 m for Pan, VNIR-SWIR and TIR bands, respectively. A Gram-Schmidt (GSSS) pan-sharpening algorithm is applied to the VNIR-SWIR bands of the Landsat-7 image to resample the multispectral data at 15-m resolution. It should be noted that many other pan-sharpening techniques have been evaluated.

Both images are processed to produce an unsupervised ISODATA classification (Iterative Self-Organizing Data Analysis Technique, Jensen 1996) on a 15-m grid. Surface emission and radiative properties are used to identify a predetermined number of surface types, referred to as elements in this study. Here, 30 and 40 elements are considered for OKC and MTL, respectively. These numbers differ for the two cities because the analysis is done with ASTER for OKC and Landsat-7 for MTL. Several problems were encountered during the data analysis. Indeed, the presence of clouds (with high reflectivity) complicates the identification of bright roofs. Moreover, it is difficult to distinguish between pixels with shallow water and shadows (related to clouds or tall buildings). Thus, in order to mitigate these problems, a partially manual processing was performed to identify the clouds and their shadows. Outside the city business center, these pixels are classified as *excluded covers*, because they are not used in the unsupervised classification. In the city business center, the tall buildings shadows are

easily extracted by using building heights information (presented in the next section). The pixels affected by this shadow problems are classified as roof if building heights are greater than 10 m.

In addition to these efforts to identify urban elements such as buildings and roads, urban green areas are also required to be reasonably well captured in the unsupervised classification process. For natural covers, our objective is to identify the main types of natural soils and vegetation in the city. Outside the city, the classification of natural soils and vegetation types is already available in the global 1-km LULC database currently used in GEM and MC2.

In all, 30 and 40 elements are identified for OKC and MTL, respectively. Some of these elements are grouped together when their spectral signatures are subjectively determined to be nearly identical and when they exhibit similar and coherent spatial distributions (according to ground truthing comparisons). Elements are finally defined, i.e., (1) *excluded covers*, (2) *water*, (3) *trees*, (4) *low vegetation*, (5) *grass*, (6) *bare soil and rocks*, (7) *roofs*, (8) *concrete*, (9) *asphalt*, (10) *vegetation and built mix 1*, and (11) *vegetation and built mix 2* (Fig. 1, first panel). The three different vegetated elements *trees*, *low vegetation*, and *grass* allow the differentiation of the green areas found in urban environments, i.e., tall trees (e.g., in the parks), mixed vegetation (composed of small trees, shrubs, and grass), and lawns (e.g., in the courtyards), respectively. By construction, the last two elements, i.e., *vegetation and built mix 1* and *vegetation and built mix 2*, are essentially mixed pixels including both impervious and natural covers. Comparison of the ASTER and Landsat-7 unsupervised classifications with aerial photographs indicates that the *vegetation and built mix 1* element is strongly correlated

with residential areas (i.e., areas composed of single-family houses) with vegetation covers (typically lawns and few trees), small roads, alleys, and individual houses. Scattered pixels of the *vegetation and built mix 2* element are located in residential areas as well, but are also observed in other urban areas. It is thus appropriate not to group these two elements together because of their distinct spatial signatures, which adds useful information for the classification.

The ASTER unsupervised classification for OKC is shown in Fig. 2. Already at this point in the classification process, the main aspects of OKC are evident in the spatial distribution of the elements. For instance, the city center (center of the study area), the two airports (south-east and south-west of the city center), the industrial districts (along the river), and the main roads are outstanding features in Fig. 2. As compared with aerial photographs, the *asphalt* category tends however to be overestimated because the classification associates most of the dark roofs with *asphalt* (because of the roofing materials or because they are wet). The impact of this confusion on the LULC classification can be reduced by using the building height database discussed in Section 2.c. As expected, Fig. 2 shows that mixing of built and vegetated elements is observed in residential areas. In these districts, the fractions and types of vegetated elements spatially vary and depend on the building density. In residential areas with large building density, *grass* is the dominant vegetation element, whereas *low vegetation* and *trees* are mainly observed in residential areas with lower building density.

c. Building height database

In this methodology, the difference between total elevation and bald Earth's topography is computed in order to obtain an estimation of the height of above-ground obstacles (i.e., the height of trees and buildings). The total elevation for OKC and MTL is obtained from the STRM-DEM database (Table 3). The bald Earth's topography comes from NED for OKC, and from CDED1 for MTL (see Table 3). Since SRTM-DEM's spatial resolution is lower than that of NED and CDED1, the SRTM-DEM database has to be resampled on NED and CDED1 grids, for OKC and MTL respectively. The grid size is 0.33 arc-second for NED and 1:50000 for CDED1. The resampling is simply done using a cubic convolution. The height of above-ground obstacles is then determined using the difference between SRTM-DEM and either NED or CDED1. And the final result, i.e., the above-ground obstacles or building heights, is interpolated using a bi-linear interpolation on the 15-m grid used for the unsupervised classification. Information on vegetation height for non-urban pixels is discarded, since our goal in this present study is to produce a strictly urban LULC database. These non-urban pixels are identified using the unsupervised classification obtained with ASTER and Landsat-7 data.

A few corrections must be applied to the resulting height field. Kellndorfer et al. (2004), in their estimation of vegetation height from SRTM-DEM and NED, observed a systematic vertical offset δ_v between the datasets. This offset can be corrected by computing the mean difference between both fields for very flat bare surfaces, i.e., without obstacles. Using about 4000 pixels for OKC and 1500 pixels for MTL, the

mean elevation difference δ_v is found to be +1.4 m for OKC and -3.0 m for MTL, with an associated standard deviation of 1.6 and 1.0 m, respectively. These offsets are subtracted from the obstacle elevations for both OKC and MTL. Moreover, all elevations smaller than a threshold value of 3 m are ignored, since they are comparable to measurement noise. This threshold also removes pixels with "obstacles" having negative elevation, such as quarries.

As shown in Fig. 3, most of the building heights are lower than 10 m, due to predominance in OKC of residential areas composed of single- or multi-family housings that do not exceed three storeys. Encouragingly, very large building heights (reaching 60 m) are found in the city center, corresponding to densely built-up areas identified by the unsupervised classification. Large values of building heights are also observed in other areas, e.g., at the airports and north as well as north-east of the city center.

It is important to realise that our objective with using this building height database is not to retrieve the height of individual buildings, but rather to assess a mean value of the urban canopy height over a larger area (i.e., about 100 m). The building-height database instead provides additional information that can be combined with the higher-resolution unsupervised classification to achieve a more realistic urban LULC classification, which is then used to initialized high-resolution atmospheric models. The enhancement resulting from the use of this building-height database is more significant for areas with tall and large buildings where building heights errors are relatively small. In low-density residential areas, however, building heights do not add much information to the classification because both vertical and horizontal resolutions are insufficient to identify low and scattered buildings.

3. Urban classification

Similarly to existing urban LULC classifications which follow the strategy outlined in Anderson et al. (1976), classes are defined in the present study based on the functionality of the urban land use types, e.g., commercial areas, housing and transportation utilities. In the next step of the classification (see Fig. 1) surface characteristics obtained from the unsupervised classification are combined with building heights to produce a final urban LULC classification. This is done following a decision tree, as described below.

a. Aggregation process

An important requirement of this study is that the urban classification must be applicable to mesoscale modeling and more specifically to urban modeling using the TEB model. The basic strategy of TEB is to parameterize urban surface processes using the concept of urban street-canyon (Oke, 1987). At each grid point of TEB's modeling domain, the ensemble of streets is represented by a single urban street canyon characterized by a set of average geometric parameters (given in Table 1, also see details in Masson, 2000).

If the urban land cover type databases are at very high resolution (i.e., with grid size small enough to resolve individual elements such as roads, buildings and parks, e.g., about 1 meter), TEB's input data could be computed for each street and each building and averaged according to the model grid resolution. Unfortunately, data used in the current study do not have sufficient horizontal resolution to achieve this. A lower

resolution database is produced here, in which a set of predetermined urban classes are defined to represent the spatial variability of the urban landscape. In this case, TEB's input data are specified by simply associating mean geometrical and physical properties to each urban class.

It is important to realise, then, that the urban classes do not represent simple elements such as roads, roofs, and lawns, but rather larger-scale urban landscapes such as residential areas, business city centers, and industrial areas. As a result, the elements obtained on the 15-m grid from the unsupervised classification, as well as the building height, have to be aggregated on a lower-resolution grid in order to identify LULC classes relevant to meteorological modeling. This aggregation step is conducted for three different target grid sizes, i.e., 60 m (4×4 pixels of the unsupervised classification), 105 m (7×7 pixels) and 195 m (13×13 pixels). The resolution of the target grid has to be determined with some care. On one hand, the aggregation process is not possible if the target grid size is too small. For instance, in the extreme case, urban landscapes can not be defined using a single 15-m element like a road or a roof. On the other hand, the classification becomes less accurate if the target grid size is too large, e.g., several urban landscapes could be present in a single pixel of the final classification.

The first step of the aggregation process is to compute the fractions of the eleven elements of the unsupervised classification for the new target grid. The first two elements (see second panel of Fig. 1), *excluded covers* and *water*, are only used as a mask to determine the coverage area of ground (natural and impervious covers), needed to calculate the relative fractions of the other nine elements (from 3 to 11). Following this procedure, the coverage fraction of *excluded covers* is calculated relative to the total

area of the pixels. Then, the coverage fraction of *water* is obtained only considering the fraction of pixels not containing *excluded covers*. Relative coverage fraction for elements 3 to 11 are computed using the total fraction of ground.

In addition to these coverage fractions of the elements of the unsupervised classification, a fraction of total built-up areas (referred to as *built* in Fig. 1) is calculated as the sum of *roofs*, *concrete*, *asphalt*, *vegetation and built mix 1*, and *vegetation and built mix 2*. Finally, building heights obtained from SRTM-DEM and NED/CDED1 are aggregated on the same target grid. This aggregation is performed only including pixels with built-up areas and elevation greater then the predetermined noise threshold (see Section 2.c), which is referred to as coverage fraction *built2*. The mean building height, on the other hand, is referred to as *height* in Fig. 1.

Thus, the aggregation results lead to fourteen classification criteria (c.f., second panel of Fig. 1): the first criteria (1 to 12 in Fig. 1) are coverage fractions directly derived from the unsupervised classification; the last two criteria (*height* and *built2*) are related to building height and density deduced using SRTM-DEM minus NED/CDED1.

b. *Decision tree model*

Our objective is to define urban classes that allow the representation of urban landscapes spatial variability required for urban modeling. To achieve this, a decision tree model is run using as inputs the coverage fractions and mean building height discussed in the previous section. In this decision tree, a sequence of logical tests is used to allocate each pixel to a specific urban class. The logical tests, given in Fig. 4, sequentially compare the coverage fractions and mean building height with

thresholds subjectively defined. Appropriate values for these thresholds are obtained in an iterative process by qualitatively evaluating results from each level of the decision tree using aerial photographs of the study domain.

The first three logical tests in the decision tree (left end of Fig. 4) isolate the pixels corresponding to *excluded covers*, *water*, and purely vegetated areas. In the lower branch of Fig. 4, natural covers are partitioned into eight vegetation classes. These include four classes for *trees*, *low vegetation*, *grass*, and *bare soil and rocks*, obtained by applying a threshold of 80% on the coverage fractions for each of these elements. For the remaining vegetation pixels that do not meet these criteria, four mixed classes are defined as combinations of vegetation types, i.e., *grass and bare soil*, *low vegetation and trees*, *low vegetation and grass*, and *trees, low vegetation and grass*.

The remaining pixels having more than 10% of built-up areas are considered as urban (upper branch of the decision tree in Fig. 4). The first identified urban class is the *roads and parking lots* class which is mainly associated with a high fraction of *asphalt* as well as a low fraction of *built2*. For pixels including buildings, with coverage fractions greater than 20% for either *built2* or *roofs*, mean building height (i.e., *height*) is tested using thresholds of 30, 20 and 10 m to identify four urban classes called *high buildings*, *mid-high buildings*, *low buildings*, and *very low buildings*. Based on comparison with aerial photographs, it is found that these four classes mainly correspond to urban landscapes with large commercial buildings or multi-family housings. Moreover, the city business center is represented by the *high buildings* class. These tests on building heights are relevant for urban modeling since urban geometric parameters vary with building height. Notably, the built-up surface areas (including both horizontal and

vertical surfaces, used for the λ_c parameter in Table 1) increases with building height and thus directly influences the heat storage process in TEB.

The decision tree model does not include any test on the coverage fraction of *concrete*, because very few pixels in either OKC or MTL include this element. It could however be useful for other cities in which the number of pixels with *concrete* is greater.

As shown in Section 2.b, the *vegetation and built mix 1* and *vegetation and built mix 2* elements are both representative of residential areas. The sum of their coverage fractions is tested in the decision tree. Beyond a cumulative fraction of 40%, the aggregated pixels are assumed to correspond to residential districts. According to the built-up density, they are subdivided in *dense residential* and *mid-density residential*.

Finally, some aggregated pixels do not correspond to any previous standard classes because of substantial mixing, which leads to some additional classes: *road mix*, corresponding to small roads mixed with vegetation or bare ground; *sparse buildings* and *low-density residential*, associated with small coverage fractions of impervious areas and buildings; and *mix of nature and built*, characterized by similar coverage fractions of vegetation and impervious areas.

Based on OKC's aerial photographs, industrial areas display very low building heights with large roof fractions. Thus, the *industrial areas* class is treated as a subclass of *very low buildings* in the decision tree (see Fig. 4). This approach is not suitable for MTL, however, since the roof signature is quite different due to the different building materials typically used in each city. Consequently, the *industrial areas* class is not generalized in the decision tree. A more advanced analysis, possibly using additional criteria, is thus required to identify this class in other cities.

c. New LULC classification

In summary, twelve new classes of urban areas (described in Table 2 and in the right panel of Fig. 1) are identified in the final classification. The 60-m resolution classifications for OKC and MTL are shown in Figs. 5 and 6, respectively. The first three urban classes listed in Table 2, corresponding to OKC and MTL city cores, exhibit similar spatial patterns. The *high buildings* class is directly associated with the central business district, which is mostly composed of skyscrapers. This class is surrounded by *mid-high buildings* and by *low buildings*.

The rest of the classification, however, is very different for the two cities. For OKC, industrial and commercial areas (associated with *mid-high buildings*, *very-low buildings*, and *industrial areas* classes) are concentrated along the main roads, whereas residential districts largely dominate elsewhere. On the other hand, MTL is much more densely built up. A large portion of the MTL northeast section and of the southeast shore is occupied by *low buildings* corresponding to contiguous multi-family housings. Elsewhere, the *dense residential* districts are predominant, whereas the *mid-density residential* and *low-density residential* classes are negligible.

As mentioned in Section 3.a, the decision tree model, initially developed by using the 60-m aggregation data, has also been tested at 105 and 195-m pixel size. The three classifications produce consistent results, in the sense that specific urban structures such as the city center, airports, or large parking lots are well identified for the three resolutions. Obviously, the elements tend to mix as the resolution decreases, which reduces the number of pixels only containing a single urban element. Not surprisingly,

the main roads are less well defined at 105 and 195-m resolution, and the building height variance is reduced (influencing the urban geometric parameters). Following this, we proceeded with the assumption that an aggregation grid of 4×4 of 15-m pixels is sufficiently large to provide realistic combinations of built and vegetated elements leading to the identification of urban classes.

d. Composition of the urban classes

The mean building height and mean composition of each urban class are shown in Fig. 7, along with the standard deviation each classification rule. The first five urban classes are associated with high cumulative fractions of *roofs*, and *asphalt* since they are mostly located in city centers and in commercial or industrial districts. The classification rule based on building height is of crucial importance for these classes, as it reduces confusion between *roofs* and *asphalt*. The *sparse buildings* is an intermediate class with a large fraction of vegetation (about 60%) and some individual buildings.

Roads is a very densely built class essentially composed of the *asphalt* element associated with a small fraction of buildings (*built2* less than 20%). The *road mix* class is much less pure than the previous one with an *asphalt* fraction of 43% and a total vegetation fraction of 38%. The composition also displays non zero fractions of *vegetation and built mix 1* and *vegetation and built mix 2*, indicating a mixing of vegetation and asphalt for some pixels. As for the *roads* class, the building heights are zero.

The built-up (or partially built-up) elements characterizing the *dense residential*, *mid-density residential* and *low-density residential* classes are mainly *vegetation and*

built mix 1 and *vegetation and built mix 2*. Fractional coverage areas of vegetation differ for each type of residential type. Quantitative assessments indicate that it is essentially the *low vegetation* element which varies the most for these classes. Lastly, the *mix of nature and built* class is only composed of 24% built-up covers (*asphalt*, *vegetation and built mix 1* and *vegetation and built mix 2*). The remaining portion of these pixels is mainly composed of *grass* and *soil and rocks*.

4. Objective evaluation of the urban land cover types

The ultimate objective of this work is to improve the representation of urban areas in atmospheric models. Unfortunately, evaluating the impact that the methodology presented here would have on surface and near-surface processes, as well as on the urban boundary layer simulated in mesoscale atmospheric models, is beyond the scope of this work and will in fact be the subject of upcoming publications.

It is expected that the accuracy of urban processes in atmospheric models strongly depends on the physical parameters that are used to initialize physical models such as TEB. Indeed, evaluating the truthfulness of parameters that describe cover fractions, geometry, as well as radiative and thermal properties of urban areas is what we seek. But as shown in Table 1, there are a large number of such parameters, even for a simple urban scheme such as TEB, and clearly systematic evaluation of these parameters over a large number of points is out of reach with the current state of knowledge (even very detailed field experiments in urban environment do not provide measurements for most of these parameters).

As explained in the Introduction, the surface physical parameters used in current atmospheric models (listed in Table 1 for TEB) are not directly based on observations (e.g., photographs, remote sensing), but are mainly obtained by association or look-up tables that provide typical values of these parameters for a certain number of land cover types. Although this is arguably not the best possible approach to specify these parameters, this represents the state of the art for high-resolution mesoscale modeling in urban environments. Therefore, the evaluation presented in this study is related to the performance of the classification methodology to identify the dominant urban cover type in single pixels, which is the final product of the approach.

To evaluate the methodology's ability to identify the main urban cover types, a set of 903 pixels from MTL's 60-m urban cover type classification was compared with high-resolution Quickbird images (60-cm pixel size, valid in Summer 2007), from which the dominant urban cover type was obtained based on photo-interpretation. The selected pixels are located on a regular grid, except for a few that were added in order to properly sample the central business district. Photo-interpretation was done by a remote-sensing specialist, using criteria similar to those depicted in Fig. 4's decision tree.

The results of this evaluation are presented in Table 4, which shows a contingency table with percentage of pixels that were correctly identified by the classification methodology. In this table, all the elements in a column add up to 100%. For example, numbers in the first column indicate that of all the pixels identified as *high buildings* in the ground truthing process with Quickbird data, 46.15% of those are indeed classified as *high buildings*, whereas 7.69% are classified as *mid-high buildings*, 38.46% are classified as *low buildings*, and 7.69% are classified as *very low buildings*.

In general, the methodology is able to capture the main urban cover types. Overall, 404 of the 903 pixels were correctly classified (i.e., about 45% of the pixels). The most significant classification confusions in this approach, apart for the one already mentioned between high and low buildings, are the following: (i) 26.67% of *mid-high buildings* pixels are classified as *low buildings*, another 26.67% are classified as *very low buildings*; (ii) 45.71% of *low buildings* are classified as *very low buildings*; (iii) 47.69% of *dense residential* pixels are classified as *very low buildings*, and iv) 23.81% of *mix of nature and built* pixels are classified as *very low buildings*, another 14.29% are classified as *dense residential*.

Based on these results, it seems the classification has a tendency to underestimate the building height, a fact that was directly verified by comparing mean building height retrieved from SRTM-DEM minus CDED1 against mean building heights retrieved from three-dimensional vectorial data (using 3277 pixels from MTL's urban cover type classification). These results, presented in Table 5, clearly shows the bias for building height retrievals. For instance, nearly 75% of 10-20 m buildings, 43.5% of 20-30 m buildings, and 27% of 30 m and taller buildings, are retrieved as *very low buildings* (which should be less than 10-m tall). Similarly, 53% of 20-30 m buildings, and 54% of 30 m and taller buildings are classified as *low buidlings* (which should be 10-20 m high).

Not surprisingly, this indicates that building height is a crucial parameter in this classification to discriminate between low and high buildings, and that the classification could be easily improved by adjusting the criteria related to height in Fig. 4's decision tree.

5. Summary and conclusions

Considering the modeling objectives and constraints that are the basis of this work, the methodology presented in this study has the advantage of using a limited number of databases readily available for the entire North America. The originality of this approach, aimed at providing descriptive urban parameters for mesoscale atmospheric models, rests on the joint analysis of satellite imagery (Landsat ETM+ and ASTER) and DEMs in order to take into account both the surface properties and the three-dimensional characteristics of the urban canopy. The application of a decision tree model results in the identification of twelve urban LULC classes and eight vegetation cover classes.

The ASTER and Landsat-7 medium-resolution satellite imagery covers large spatial areas and is available free of charge or at low cost in addition of providing consistent element classifications. Obviously, the method is not perfect and has several weaknesses. For instance, the roofs are sometimes poorly retrieved. Also, the vegetation signature strongly depends on the season when the satellite image was collected. During summertime, the trees can obstruct the observation of houses and roads in residential areas, leading to an underestimation of built-up covers.

The other databases used in the methodology, related to building height and bald Earth topography, have relatively low spatial resolution. Their horizontal and vertical resolutions are insufficient to extract the individual buildings and to identify one-storey buildings. Nevertheless, different types of districts can be distinguished according to the mean building height retrievals from SRTM-DEM and NED/CDED1 databases.

Notably, the business city center is always very well identified using this technique, in spite of the significant underestimation of building height which was evidenced by comparison against detailed three-dimensional vector data over MTL. This bias was shown to lead to some confusion between low buildings, mid-high buildings, and high buildings.

Even though each type of data has its limitations, their coupling in the decision tree makes it possible to improve the quality of the analysis results and to better characterize the urban land cover types. The methodology is automated as much as possible but some manual processing is still necessary. Indeed, manual intervention is still required regarding problems related to shadow and cloud cover effects in the ASTER and Landsat-7 imagery and to the systematic offset observed between SRTM-DEM and NED/CDED1.

The study of OKC, MTL and more recently Vancouver (BC, Canada) (not presented here) allowed the refinement and standardization of the decision tree. The general and robust approach has been found to lead to a satisfying identification of the major urban landscapes of North American cities. It is worth noting that the three chosen cities are quite different in terms of size, arrangement of districts, types of buildings, and materials. The spatial resolution and the number of urban classes are well adapted to microscale ($\simeq$ 200 m) and mesoscale ($\simeq$ 1 km) modeling and provide an appropriate representation of the spatial urban land cover type variability.

It should be noted, to conclude, that future studies should aim at directly retrieving urban parameters required for urban modeling. Although not simple, this may be possible for geometric parameters (street width, building height) and fractional coverage

areas (e.g., built versus vegetated areas). Other parameters related to radiative and thermal properties of urban materials are certainly more difficult to obtain, at least using remote sensing approaches. Effort in this direction is nevertheless necessary, since these parameters have a considerable impact on the urban microclimate and on the local meteorology. The development of new approaches and new methods, based on analysis of high resolution satellite images and ancillary data, will represent a major field of research for the next years.

Acknowledgments. The authors are grateful to Jean-Philippe Gauthier and Louise Blais for their assistance. The support of MSC management, in particular Michel Jean, Richard Hogue, and Gilbert Brunet, is warmly acknowledged. This work was funded by the Chemical, Biological, Radiological and Nuclear (CBRN) Research and Technology Initiative (CRTI) (Project #02-0093RD) of Defence R&D Canada.

References

Anderson, J., E. Hardy, J. Roach, and R. Witmer, 1976: *A Land Use and Land Cover Classification System for Use with Remote Sensor Data*. U.S. Government Printing Office, Washington D.C., USA.

Bélair, S., L.-P. Crevier, J. Mailhot, B. Bilodeau, and Y. Delage, 2003: Operational implementation of the ISBA land surface scheme in the Canadian regional weather forecast model. Part I: Warm season results. *J. of Hydrometeorol.*, **4**, 352-370.

Burian, S., M.J. Brown, J.K.S. Ching, M.L. Cheuk, M. Yuan, W. Han, and A.T. McKinnon, 2004: *Urban morphological analysis for mesoscale meteorological and dispersion modeling applications: Current issues*. American Meteorological Society, Fifth Conference on Urban Environment, Vancouver, BC, Canada, Abstract 9.1.

Danko, D. M., 1992: The digital chart of the world. *GeoInfo Systems*, **2**, 29-36.

De Jong, S. M., A. Bagré, P.B.M. van Teeffelen, W.P.A. van Deursen, 2000: Monitoring Trends in Urban Growth and Surveying City Quarters in the City of Ouagadougou, Burkina Faso Using SPOT-XS. *Geocarto International*, **15**(2), 61-68.

Friedl, M. A., D.K. McIver, J.C.F. Hodges, X.Y. Zhang, D. Muchoney, A.H. Strahler, C.E. Woodcock, S. Gopal, A. Schneider, and A. Cooper, 2002: Global land cover mapping from MODIS: algorithms and early results. *Remote Sensing of Environment*, **83**(1-2), 287-302.

Gamba, P., F. Dell'acqua, B. Houshmand, 2002: *SRTM data characterization in urban areas*. ISPRS Commission III Symposium on Photogrammetric Computer Vision, Graz, Austria, XXXIV(3B), 55-58.

Grimmond, C.S.B., and C. Souch, 1994: Surface description for urban climate studies: a GIS based methodology. *Geocarto International*, **9**, 47-59.

Grimmond, C.S.B., and T.R. Oke, 1999: Aerodynamic properties of urban areas derived from analysis of surface form. *J. Appl. Meteorol.*, **38**, 1262-1292.

Guidon, B., Y. Zhang, and C. Dillabaugh, 2004: Landsat urban mapping based on a combined spectral-spatial methodology. *Remote Sensing of Environment*, **92**, 218-232.

Hansen, M.C., R.S. DeFries, J.R.G. Townshend, and R. Sohlberg, 2000: Global land cover classification at 1 km spatial resolution using a classification tree approach. *Int. J. Remote Sensing*, **21**, 1331-1364.

Heymann, Y., and Coauthors, 1993: *CORINE land cover: Technical guide*. Environment, nuclear safety and civil protection series, Commission of the European Communities, Office for Official Publication of the European Communities, Luxembourg, 144pp.

Kellndorfer, J.M., W.S. Walker, L.E. Pierce, M.C. Dobson, J. Fites, C. Hunsaker, J. Vona, and M. Clutter, 2004: Vegetation height derivation from Shuttle Radar Topography Mission and National Elevation data sets. *Remote Sensing of Environment*, **93**(3), 339-358.

Kondo, H., and F. Liu, 1998: Study onthe Urban Thermal Environment Obtained through One-Dimensional Urban Canopy Model. *Journal of Jpn. Soc. Atmos. Environ.*, **33**(3), 179-192 (in Japanese with English abstract).

Kusaka, H., H. Kondo, Y. Kikegawa, and F. Kimura, 2001: Simple Single-Layer Urban Canopy Model for Atmospheric Models: Comparisonwith Multi-Layer and Slab Model. *Boundary-Layer Meteorol.*, **101**, 329-358.

Loveland, T.R., B.C. Reed, J.F. Brown, D.O. Ohlen, Z. Zhu, L. Yang, and J.W. Merchant, 2000: Development of a global land cover characteristics database and IGBP DISCover from 1 km AVHRR data. *Int. J. Remote Sensing*, **21**(6-7), 1303-1330.

Lu, D., and Q. Weng, 2004: Spectral Mixture Analysis of the Urban Landscape in Indianapolis with Landsat ETM+ Imagery. *Photogrammetric Engineering and Remote Sensing*, **70**(9), 1053-1062.

Mailhot, J., S. Bélair, A. Lemonsu, L. Tong, A. Leroux, N. Benbouta, and R. Hogue, 2006: Urban modeling at the Meteorological Service of Canada. *International Association for Urban Climate (IAUC) Newsletter*, **17**, 13-16 (available online at *http://www.urban-climate.org*).

Martilli, A., A. Clappier, and M.W. Rotach, 2002: An urban surface exchange parameterization for mesoscale models. *Boundary-Layer Meteorol.*, **104**, 261-304.

Masson, V., 2000: A physically-based scheme for the urban energy budget in atmospheric models. *Boundary-Layer Meteorol.*, **94**, 357-397.

Mills, G., 1997: An urban canopy-layer climate model. *Theoretical and Applied Climatology*, **57**, 229-244.

Noilhan, J., and S. Planton, 1989: A Simple Parameterization of Land Surface Processes for Meteorological Models. *Mon. Wea. Rev.*, **117**, 536-549.

Oke, T. R., 1987: *Boundary Layer Climates*. 2nd edition, Methuen, London, 435pp.

Oke, T. R., 2004: *Initial Guidance to Obtain Representative Meteorological Observations at Urban Sites*. Instruments and Methods of Observation Program, IOM Report No. 81, WMO/TD 1250, World Meteorological Organization, Geneva, Switzerland.

Ramsey, M. S., 2003: *Mapping the city landscape from space: The Advanced Spaceborne Thermal Emission and Reflectance Radiometer (ASTER) Urban Environmental Monitoring Program*. In Heiken, G., R. Fakundiny, and J. Sutter (eds.), Earth Science in the City: A Reader, American Geophysical Union, pp. 337-361.

Ridd, M. K., 1995: Exploring a V-I-S (vegetation-impervious surface-soil) model for urban ecosystem analysis through remote sensing: comparative anatomy for cities. *Int. J. Remote Sens*, **16**, 2165-2185.

Stefanov, W.L., M.S. Ramsey, and P.R. Christensen, 2001: Monitoring urban land cover change: An expert system approach to land cover classification of semiarid to arid urban centers. *Remote Sensing of Environment*, **77**, 173-185.

Vogelmann, J.E.,S.M. Howard, L. Yang, C.R. Larson, B.K. Wylie, and N. van Driel, N., 2001: Completion of the 1990s national land cover data set for the contermi-

nous United States from Landsat Thematic Mapper data and ancillary data sources. *Photogrammetric Engineering and Remote Sensing*, **67**, 650-662.

Zhang, Y., and B. Guindon, 2005: *Using Landsat data to assess land use conversion impacts arising from urbanization: The Canadian context*. 5th International Symposium on Remote Sensing of Urban Areas (URS 2005), Tempe, AZ, USA.

List of Tables

List of Figures

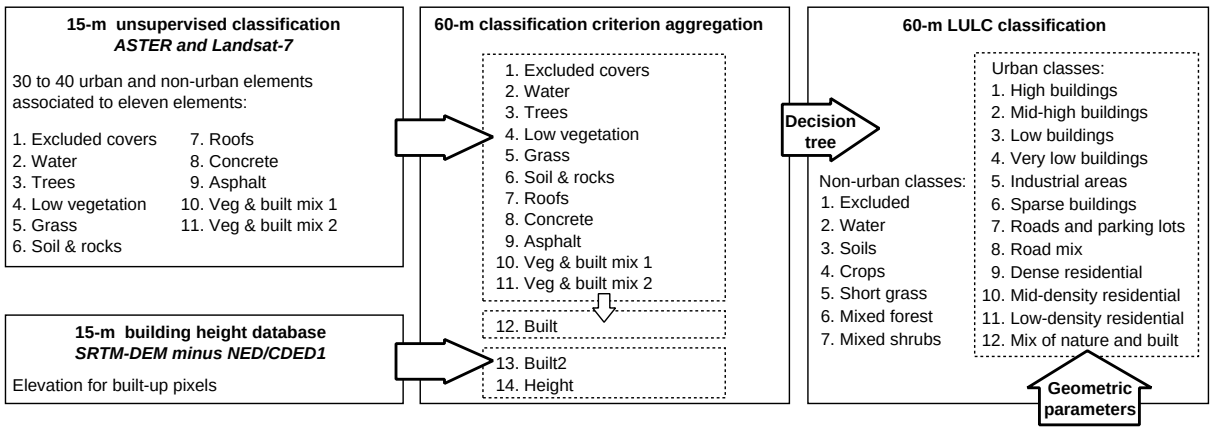

FIG. 1. : General description of the methodology.

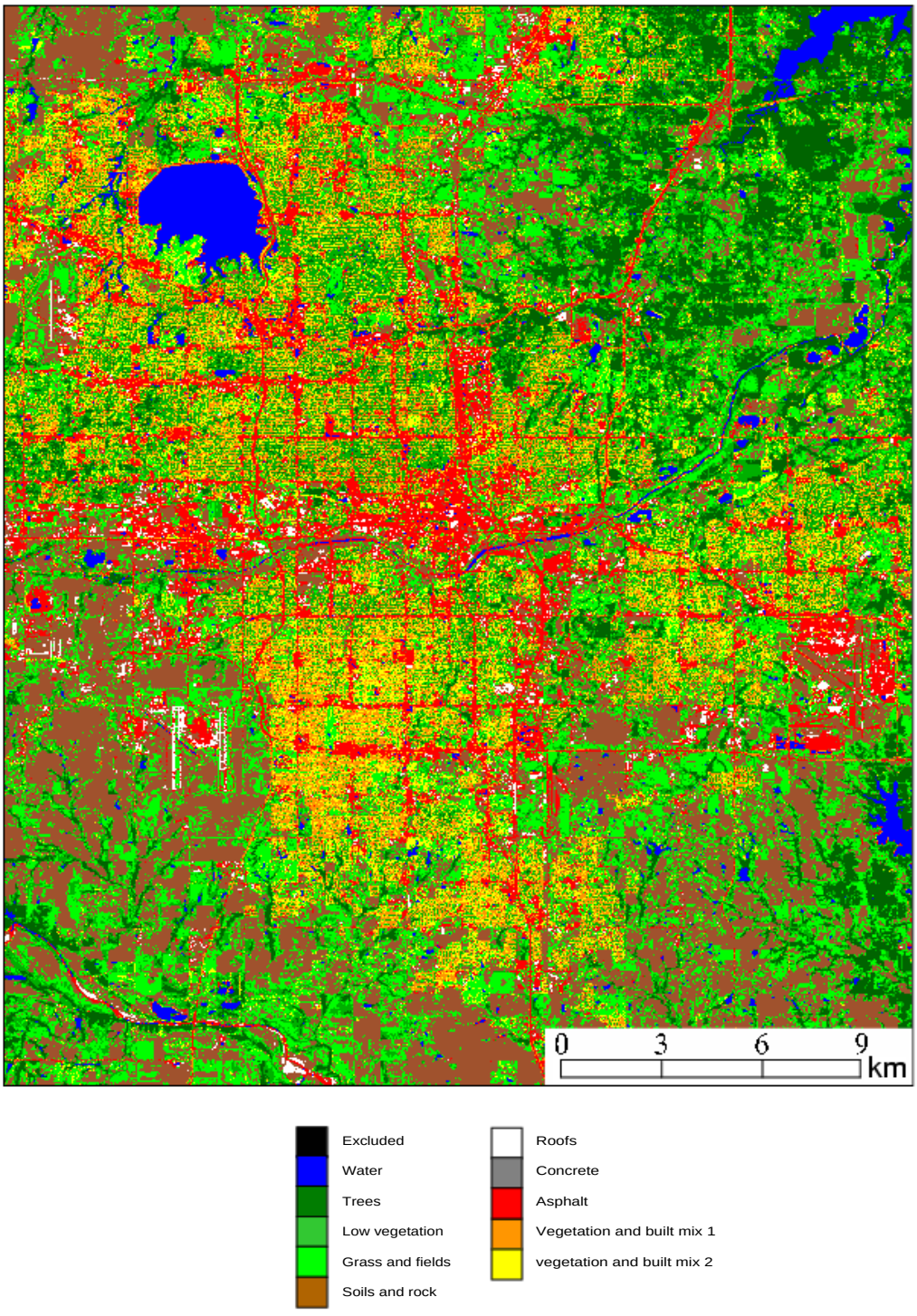

FIG. 2. : Unsupervised classification of ASTER satellite imagery for OKC.

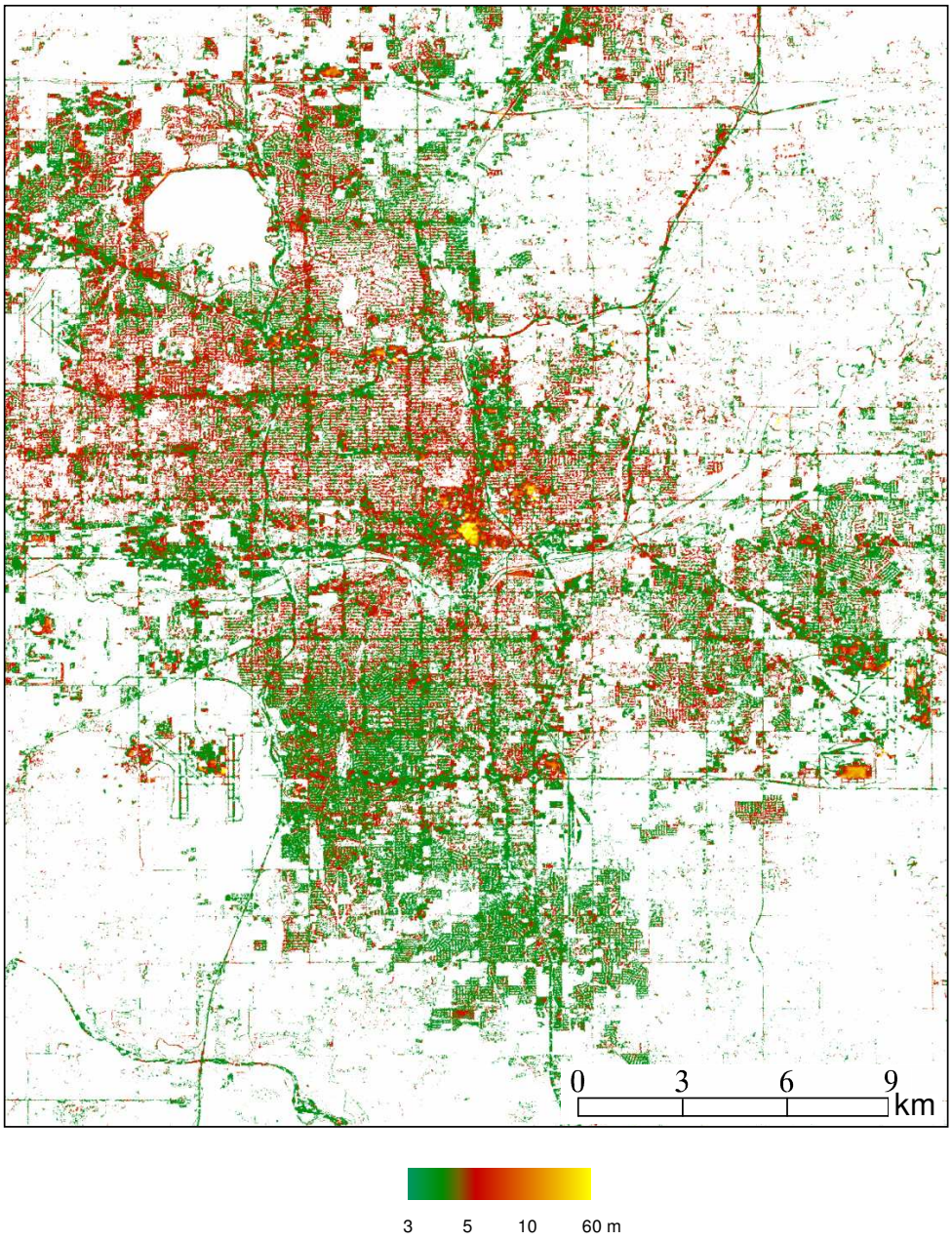

FIG. 3. : Estimation of building heights resulting from SRTM-DEM minus NED/CDED1 databases for OKC. White areas correspond to the pixels not considered as built-up pixels or where the difference field is less than the threshold (i.e., 3 m).

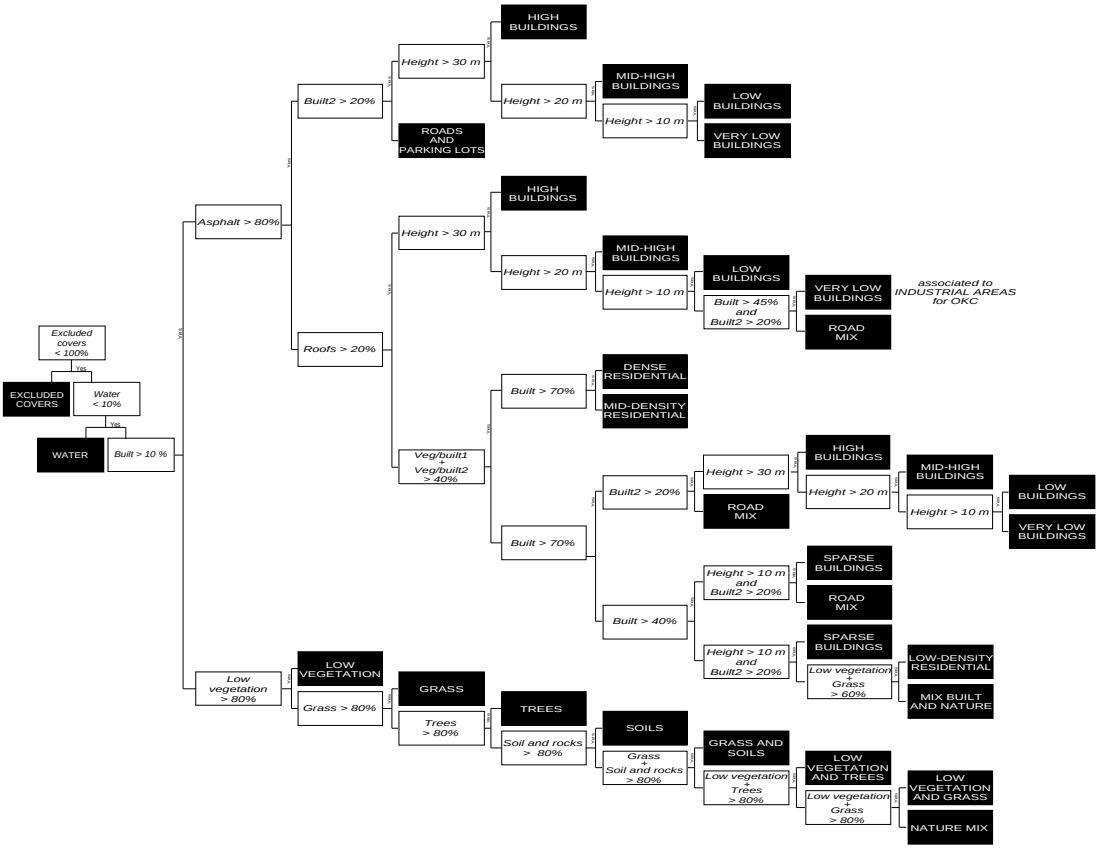

FIG. 4. : Decision tree model applied to the 60-m element databases by using the fourteen selection criteria defined in Section 3.a.

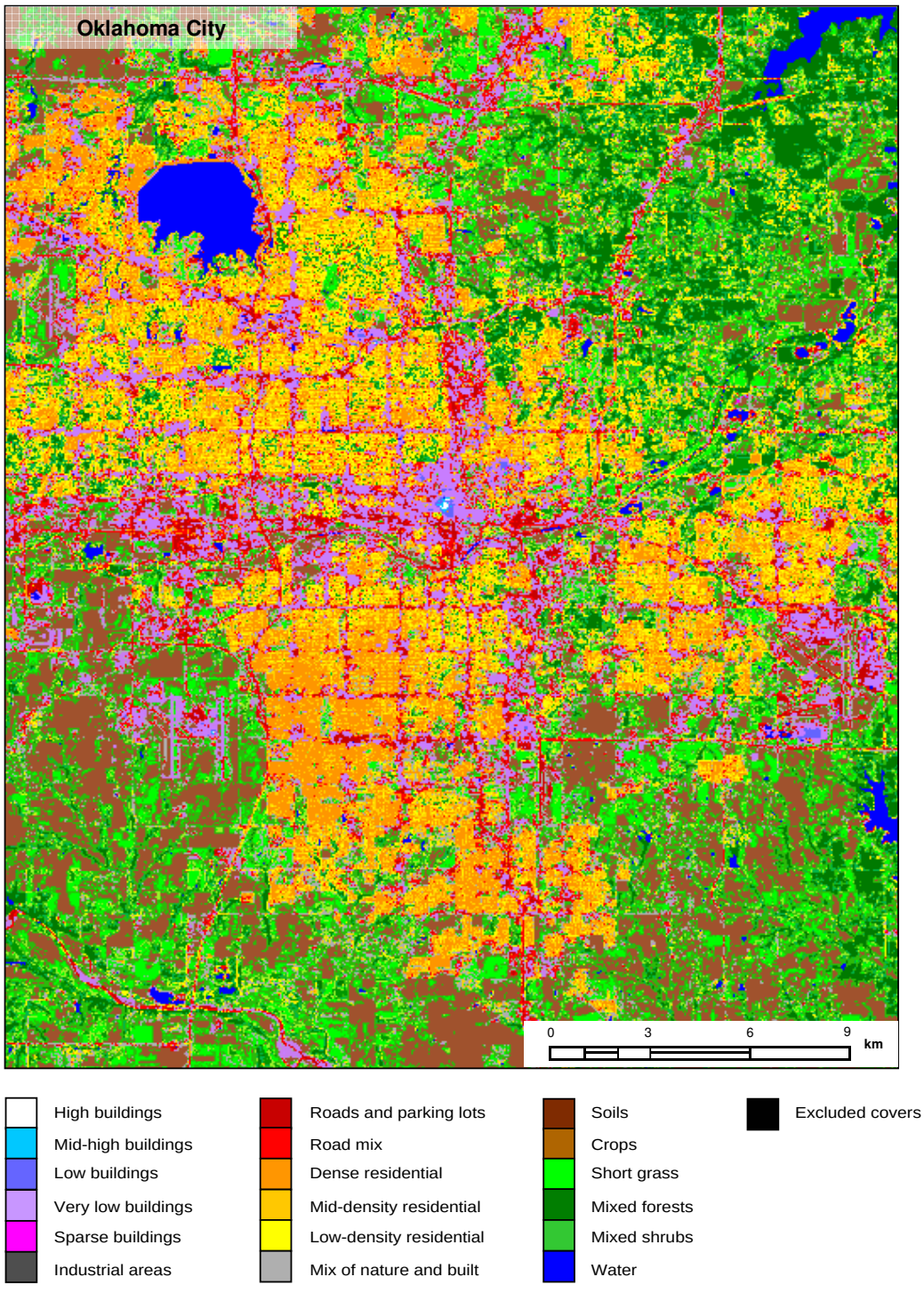

FIG. 5. : Final LULC 60-m classification of OKC including the twelve new urban classes and five classes of natural covers already defined in the global classification.

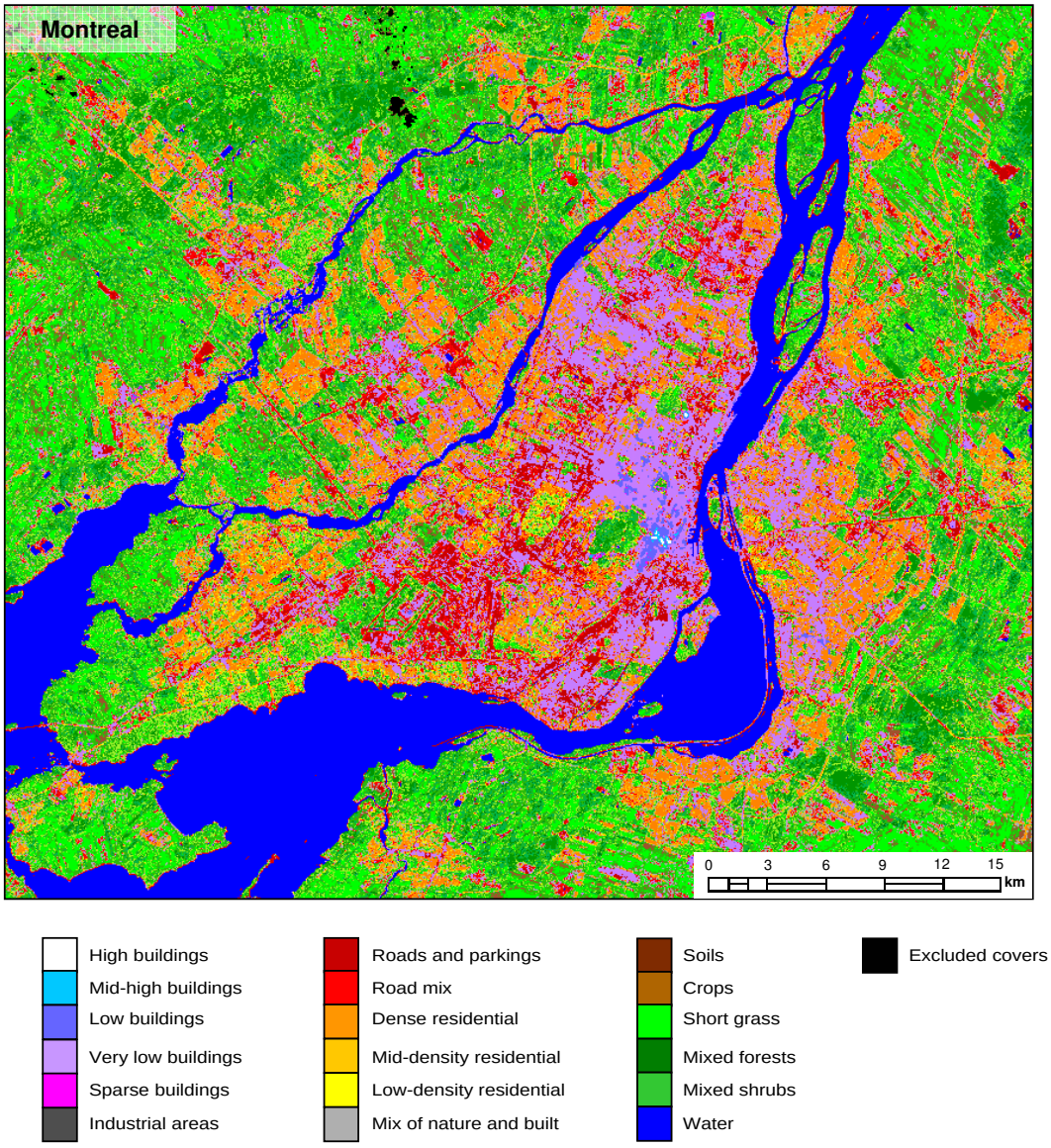

FIG. 6. : Final LULC 60-m classification of MTL including the twelve new urban classes and five classes of natural covers already defined in the global classification.

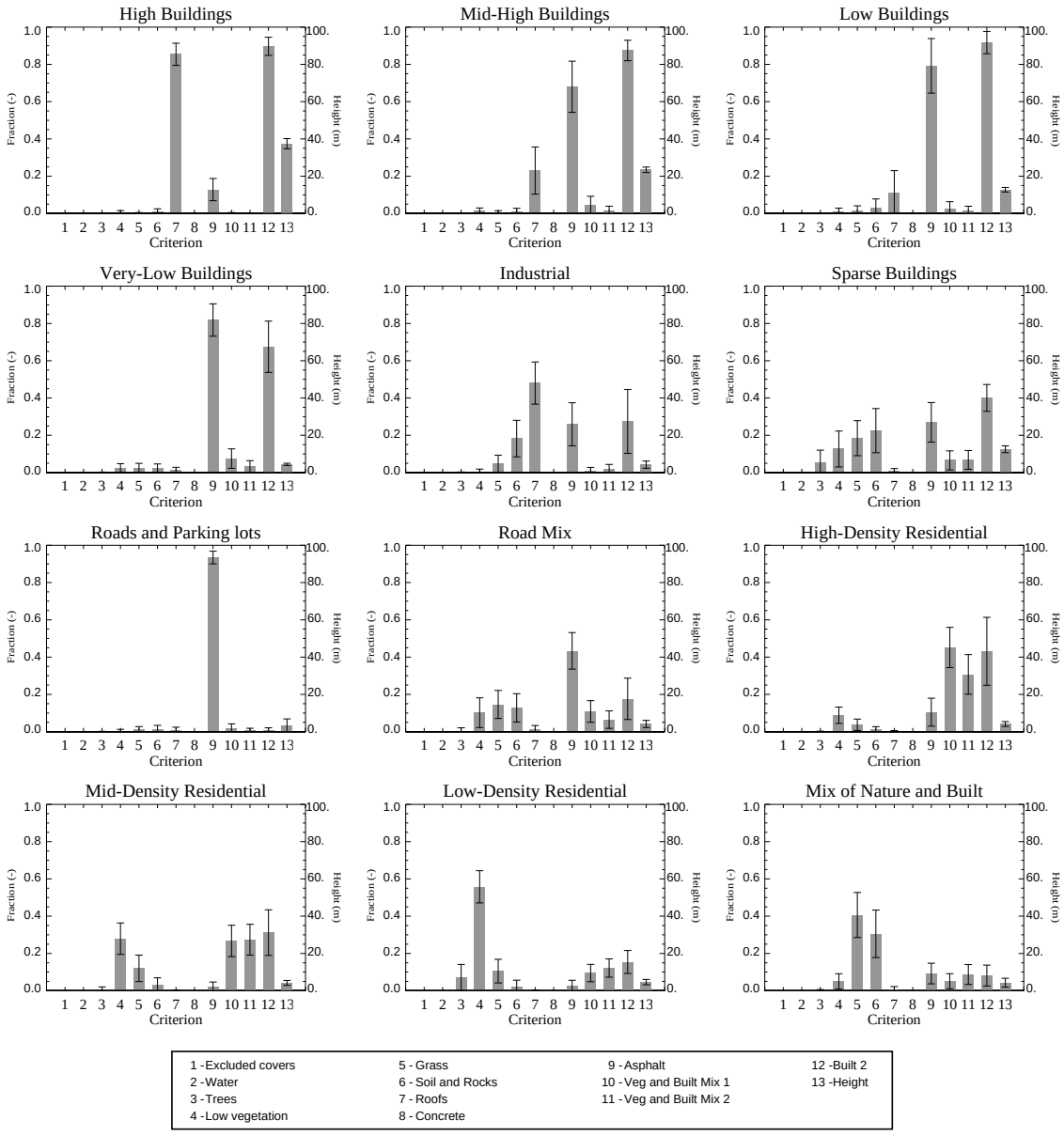

FIG. 7. : Composition of the twelve urban classes showing the averaged values of each classification criterion and the associated standard deviations. Except for the mean building height (last criterion) expressed in m, all the criteria correspond to fractions.

TABLE 1. : Cover fractions and TEB input parameters (see Masson, 2000) required for modelling applications.

Parameters	Description	Unit
Cover fractions		
f_{built}	Built-up cover fraction	-
f_{trees}	Tree fraction	-
f_{grass}	Grass fraction	-
f_{soil}	Bare soil fraction	-
TEB input parameters		
Geometric parameters		
f_{bld}	Building fraction	-
z_{bld}	Mean height of buildings	m
z_{0m}	Aerodynamic roughness length	m
λ_c	Wall/horizontal area ratio	-
z_{bld}/W	Canyon aspect ratio	-
Radiative properties		
α_{roof}	Roof albedo	-
α_{road}	Road albedo	-
α_{wall}	Wall albedo	-
ϵ_{roof}	Roof emissivity	-
ϵ_{road}	Road emissivity	-
ϵ_{wall}	Wall emissivity	-
Thermal properties		
d_{roof}	Roof layer thickness	m
λ_{roof}	Thermal conductivity of roof layers	W m^{-1} K^{-1}
C_{roof}	Heat capacity of roof layers	J m^{-3} K^{-1}
d_{road}	Thickness of road layers	m
λ_{road}	Thermal conductivity of road layers	W m^{-1} K^{-1}
C_{road}	Heat capacity of road layers	J m^{-3} K^{-1}
d_{wall}	Thickness of wall layers	m
λ_{wall}	Thermal conductivity of wall layers	W m^{-1} K^{-1}
C_{wall}	Heat capacity of wall layers	J m^{-3} K^{-1}

TABLE 2. : Description of the twelve urban classes derived from the decision tree classification. The last column presents the relation between the urban classes, defined here, and the urban climate zones (UCZs) proposed by Oke (2004).

	Urban classes	Characteristics	UCZ
1.	High buildings	*City business center; high-rise buildings*	1
2.	Mid-high buildings	*Commercial buildings and multi-family housings*	2
3.	Low buildings	*Commercial buildings and multi-family housings*	2
4.	Very low buildings	*Commercial buildings and multi-family housings*	3
5.	Industrial areas	*Majority of large warehouses*	4
6.	Sparse buildings	*Large individual buildings*	-
7.	Roads and parking lots	*Main roads and large parking lots*	-
8.	Road mix	*Mix of roads and vegetation*	-
9.	Dense residential	*Contiguous single-family housings*	5
10.	Mid-density residential	*Single-family housings with lawns*	6
11.	Low-density residential	*Single-family housings with large lawns*	7
12.	Mix of nature and built	*Mix of various urban types*	-

TABLE 3. : References and characteristics of the various source data.

Type	Spatial Resolution	Source	Date
Aerial photos	0.3 m	USGS[1]	2002-03-26 (OKC)
ASTER L1B	15 m (VNIR), 30 m (SWIR), 90-m (TIR)	USGS	2001-07-21 (OKC)
Landsat-7	15 m (Pan), 30 m (VNIR-SWIR), 60 m (TIR)	UMD's GLCF[2]	2001-06-08 (MTL)
NED	1/3 arc-sec over US	USGS	1998 and 2001
CDED1	1:50000 over Canada	NRCan[3]	1995-1999
SRTM-DEM	1 arc-sec (US), 3 arc-sec (World)	UMD's GLCF	February 2000

[1] US Geological Survey

[2] University of Maryland's Global Land Cover Facility

[3] National Resources Canada

TABLE 4. : Contingency table presenting the percentage of pixels that are correctly identified by the classification methodology after comparison against high-resolution Quickbird images for MTL.

CLASSES \ GROUND TRUTH	High buildings	Mid-high buildings	Low buildings	Very low buildings	Industrial areas	Sparse buildings	Roads and parking lots	Road mix	Dense residential	Mid-density residential	Low-density residential	Mix of nature and built	Low vegetation and grass	Low vegetation and trees	Grass and soil	Nature mix	Water
High buildings	46.15	0.	0.	0.	0.	0.	0.	0.	0.	0.	0.	0.	0.	0.	0.	0.	0.
Mid-high buildings	7.69	20.00	0.	0.	0.	0.	0.	0.	0.	0.	0.	0.	0.	0.	0.	0.	0.
Low buildings	38.46	26.67	25.71	1.82	0.	0.	0.	0.	4.17	0.	0.	2.38	0.	0.	0.	0.	0.
Very low buildings	7.69	26.67	45.71	78.18	0.	100.00	50.00	32.76	47.69	16.49	0.	23.81	0.	0.	5.26	0.	0.
Industrial areas	0.	0.	0.	0.	0.	0.	0.	0.	0.	0.	0.	0.	0.	0.	0.	0.	0.
Sparse buildings	0.	0.	0.	0.	0.	0.	0.	0.	0.	1.03	0.	0.	3.85	0.	0.	0.	0.
Roads and parking lots	0.	6.67	14.29	13.64	0.	0.	30.00	15.52	5.09	1.03	0.	2.38	0.	0.	5.26	0.	0.98
Road mix	0.	6.67	11.43	3.64	0.	0.	10.00	43.10	3.70	7.22	0.	10.32	0.	6.67	10.53	17.95	0.98
Dense residential	0.	6.67	0.	0.91	0.	0.	0.	6.90	34.72	44.33	0.	14.29	3.85	0.	10.53	0.	0.
Mid-density residential	0.	0.	0.	0.	0.	0.	5.00	1.72	3.24	16.49	20.00	9.52	0.	0.	5.26	0.	0.
Low-density residential	0.	0.	0.	0.91	0.	0.	0.	0.	0.46	3.09	20.00	7.14	0.	6.67	0.	7.69	0.
Mix of nature and built	0.	6.67	0.	0.	0.	0.	0.	0.	0.46	9.28	0.	18.25	0.	6.67	0.	5.13	0.
Low vegetation and grass	0.	0.	0.	0.	0.	0.	0.	0.	0.	0.	0.	1.59	57.69	0.	5.26	10.26	0.
Low vegetation and trees	0.	0.	0.	0.	0.	0.	0.	0.	0.46	0.	30.00.	3.17	11.54	46.67	0.	2.56	0.
Grass and soil	0.	0.	0.	0.	0.	0.	0.	0.	0.	0.	10.00	0.79	3.85	20.00	47.37	0.	0.
Nature mix	0.	0.	2.86	0.91	0.	0.	5.00	0.	0.	1.03	20.00	6.35	19.43	13.33	10.53	56.41	0.
Water	0.	0.	0.	0.	0.	0.	0.	0.	0.	0.	0.	0.	0.	0.	0.	0.	98.04

TABLE 5. : Contingency table presenting the percentage of pixels of the urban classes *high buildings*, *mid-high buildings*, *low buildings*, and *very low buildings* for which building heights are correctly retrieved by STRM-DEM minus CDED1 after comparison against three-dimensional vectorial data for MTL.

CLASSES	GROUND TRUTH: + 30 m	20 - 30 m	10 - 20 m	0 - 10 m
High buildings	6.90	1.16	0.16	0.09
Mid-high buildings	12.03	2.55	0.47	0.
Low buildings	53.90	52.78	24.39	8.39
Very low buildings	27.17	43.52	74.98	91.53